

# From Network to Rover: Near Real-Time PPP Solution with Ambiguity Resolution

P. Sarri, K. Y. Kouedjin, D. Gallego Maya, R. Zaid, A. Guinamard

*SBG-Systems SAS - 1 avenue Eiffel - 78420 - Carrières-sur-Seine - France*

## KEY WORDS

Precise Point Positioning, Ambiguity Resolution, Uncalibrated Phase Delay, Fractional Cycle Bias

## ABSTRACT

While Precise Point Positioning with Ambiguity Resolution (PPP-AR) has become a major tool in multi-constellation Global Navigation Satellite System (GNSS), a critical component to enable it is the generation of satellite phase biases. Several analysis centers (AC) under International GNSS Service (IGS) have developed services to generate PPP-AR products including phase bias corrections with a typical delay reaching several days. Another significant challenge is the lack of interoperability between the various corrections streams and rover PPP engines, each one having a different error model. Current and emerging applications need not only the centimeter precision provided by the PPP-AR but also the availability merely hours after the mission is accomplished. Finally, an end-to-end solution, capable of both generating corrections and computing the user position to the centimeter level, is a key to addressing a non-expert audience.

This paper aims to present an innovative solution that guarantees the end user a centimeter-level position in near real-time. The in-house solution is responsible for the entire processing chain including the estimation of satellite phase biases which are needed for integer ambiguity resolution (AR) in PPP, and the user-side PPP-AR position computation. The major advantage of our solution is the ability to provide corrections less than one hour after the mission, thus enabling new applications. Initial results of the designed estimator showed great stability of the Uncalibrated Phase Delays (UPDs). The latter when infused into our PPP solution produced a centimetric position.

## I. INTRODUCTION

Over the years, the Precise Point Positioning technology has proved to be an excellent choice to reach centimeter absolute precision, while suffering from long convergence time [1]. To speed up its convergence time and provide a high precision solution for PPP, Ambiguity Resolution was introduced [2]. In general, the ambiguity loses its integer property due to the inclusion of satellite and receiver biases. These biases originate from the instrumental delays in GNSS signal generation and processing chain. A wide range of studies has been done concerning the Uncalibrated Phase Delays estimation, AR method, performance and its applications [2] [3]. Nowadays, with the rapid changes in GNSS, more frequency observations and constellations are available; thus, we expect PPP-AR to improve [4]. One key factor to achieving multi-GNSS and multi-frequency PPP-AR, is the need of multi-frequency UPD products for all available constellations to recover the integer part of each ambiguity [5].

To compute and dissociate the lumped biases, several methods were proposed with a starting point being the collection of data from a global network of base stations. After the aggregation of data, we started by computing float ambiguities depending on the type of PPP model that is run. Then, we estimated the UPDs based on an Iterative Least Squares method [6] [7] in conjunction with a smart engine that separates outliers from valid ambiguities. The near real-time UPDs are provided at a sampling rate of 30 seconds on a 15-minute block with a latency of an hour; thus, termed near real-time. These constraints were due to the availability of data required for the entire processing chain. However, results showed that an hour latency was still enough to provide accurate positioning and fast convergence due to the nature of the UPDs. A globally distributed network consisting of about 100 IGS stations is selected. Due to the real-time nature, the number of stations varies over time as well as the data per station. Despite these variations, the quality of the UPDs were not affected.

This paper focuses on the novelty the in-house solution brings. The estimated quality of GPS and Galileo UPDs and the positioning performance of multi-GNSS PPP-AR is completely evaluated. We give a detailed explanation of the entire server-level architecture. Some base stations used as control are tested. Finally, conclusions and future perspectives are given.

## II. METHODOLOGY

The proposed in-house solution is divided in four main modules. First, the Download Manager keeps a permanent connection with multiple FTP and NTrip servers. This redundancy in the data providers is essential to guarantee the availability of the input data. If a precise server is in maintenance or becomes unavailable, the solution will continue to run by downloading the information from the backup servers. It is important to note that the data of a vast network of base stations is needed. Everything is downloaded as soon as it becomes available in the servers, allowing a near-real time processing for the entire solution. Finally, the dual FTP/NTrip enables future proof real time operation.

The second module is in charge of the float ambiguity estimation. Multiple parallel processing of a float PPP algorithm are used to estimate the float ambiguities of all the base stations as fast as possible. In this module, the integrity of the estimated ambiguities is monitored, using several fault detection and rejection methods to provide the best quality estimations to the next module.

The next module is the UPDs Estimation. The first part of this module will analyze the stability of the previously estimated float ambiguities. All the ambiguities from all the base stations that have sufficiently converged are added to the network algorithm that will estimate the uncalibrated phase biases. In order to separate the receiver fractional bias from the satellite one, a reference base station must be selected within the network.

Finally, a quality control and integrity monitoring of the generated UPD values is executed in the last module. A subset of base stations is selected to run a PPP-AR processing using the estimated values. At this stage, not only the estimated position is compared with a high precision reference, but also the satellite information and the ambiguity status are monitored.

Figure 1 presents the overview of the proposed solution. The following section will present each module in more detail.

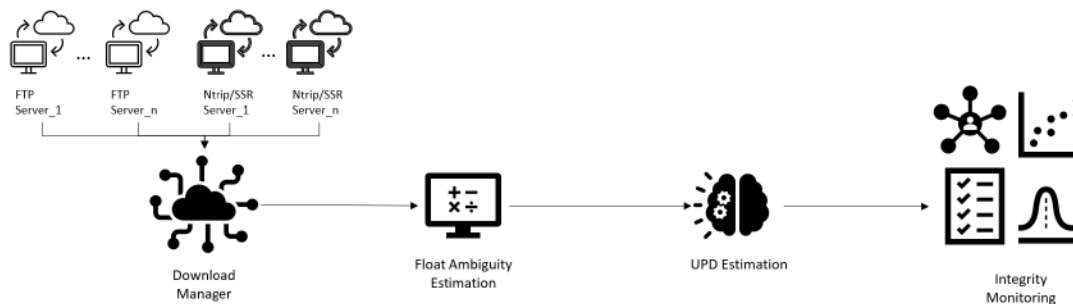


**Figure 1:** Overview of the proposed solution

### 1. Download Manager

We need a selection of high quality stations, with low occurrences of GNSS disruptions, well spread over the world as shown in Figure 2. All data needed to estimate the UPDs are downloaded with this module. The files downloaded include the observation data from Multi-GNSS Experiment (MGEX), Antenna Exchange file (ANTEX), Differential Code Bias (DCB), Orbits and Clock. The observation files are provided for a 15-min period; thus, the entire processing is done at a 15-min interval. To prevent data loss and downtime, server redundancy was implemented as data from various servers and NTRIP streams are collected.

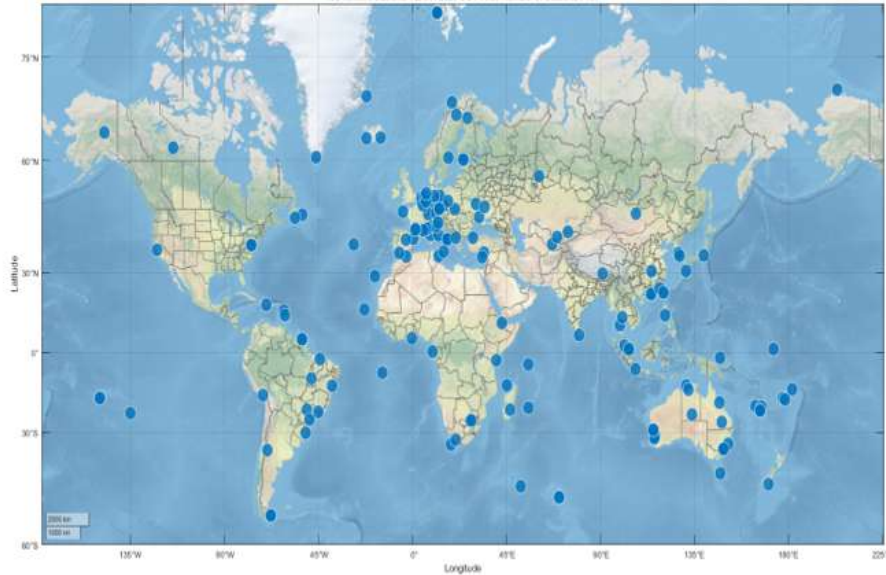


**Figure 2:** Base Stations Network

## 2. Float Ambiguity Module

With the aggregated data from the download manager, clean observations are processed by different Kalman filter contexts (one per station running in parallel) [8]. The outputs of each Kalman context serve as input to the final stage. Although it may represent a significant CPU overhead, all observations are processed at 1Hz to optimize the performance of float ambiguities computation.

## 3. UPD Estimation Module

From the previously computed float ambiguities, several checks are performed in order to select the best float ambiguities before running the estimator. These checks are to qualify each set of ambiguities in order to speed up the convergence of the UPDs estimator. Once validated and the UPDs estimated, the residuals for all used ambiguities during the computation are calculated as a mean to check the accuracy of the products. The estimator has been designed to cope with any type of ambiguities, such as ionosphere free ambiguities or zero combination ambiguities.

### *Uncalibrated Phase Delays Estimation*

The UPD estimation method applies to any type of float ambiguities that have been validated before the computation. The float ambiguity can be written as:

$$N_r^s = [N_r^s] + b_r - b^s \quad (1)$$

Where:

- $N_r^s$  is the float ambiguity
- $[N_r^s]$  is the integer part of the float ambiguity
- $b_r$  is the station receiver phase bias
- $b^s$  is the satellite phase bias

By using a global network of base stations, the phase biases can be estimated with an iterative Least Squares method [6] [9] [10] [11]. To separate the satellite bias from the base station bias, a station is selected as a reference with its corresponding bias set to zero.

Assuming that  $m$  satellites are tracked by a network of  $n$  stations, the UPD estimation equation ( $Y = H \cdot x$ ) can be formulated as follows:

$$\begin{bmatrix} N_1^1 - [N_1^1] \\ N_1^2 - [N_1^2] \\ \vdots \\ N_1^m - [N_1^m] \\ \vdots \\ N_n^1 - [N_n^1] \\ \vdots \\ N_n^m - [N_n^m] \end{bmatrix} = \begin{bmatrix} -I_m & & \\ & \ddots & \\ & & -I_m \end{bmatrix} S_n \cdot \begin{bmatrix} b^1 \\ \vdots \\ b^m \\ b_1 \\ \vdots \\ b_n \end{bmatrix} \quad (2)$$

where:

- $I_m$  is the identity matrix of size  $m * m$
- $S_n$  is a matrix of  $m * n$  rows and  $n$  columns
- 

$$S_n = \begin{bmatrix} A_1 & \dots & 0 \\ \vdots & \ddots & \vdots \\ 0 & \dots & A_1 \end{bmatrix}$$

- with

$$A_1 = [1 \quad 1 \quad \dots \quad 1]^T$$

#### 4. Integrity Monitoring

Finally, the quality control module is a very important added value of the proposed solution. In this module, the quality and integrity of the estimated products are monitored in near real time. This element is crucial in providing the end user with useful information about the global network status, and the health status of each individual satellite. Moreover, it also provides historical data that plays a key role in the validation, debugging and improvement phases.

The first part of the quality control is based on the constant monitoring of the stability of the estimated values, as well as their standard deviation and the number of base stations used for each estimation. Additionally, the float-fix residual of each ambiguity is periodically studied to ensure less of a quarter of a cycle difference. The global network is also inspected, as a well spread network covering as much territory as possible is the needed scenario to guarantee the global compatibility of the products. The second part of the quality control concerns the direct use of the proposed products. For this, a subset of base stations is selected to run a PPP-AR processing in the same way an end-user is expected to do. For this control network, the precise position is previously known, so the position error is monitored to confirm a centimeter-level precision. Finally, the PPP product quality is evaluated along with satellite health : If the sub-network stations are able to fix one satellite ambiguities, we can put more trust on the generated products and overall satellite quality. On the contrary, recurrent rejection or high residual on a specific satellite is a clear indication of a bad satellite health. The satellite health status is part of the generated product. It is important to mention that the quality control and integrity monitoring is executed as soon as new products are estimated in order to satisfy the near real-time constraint.

### III. RESULTS

#### 1. UPD WL GPS

Figure 3 shows the results of a near real-time processing of the Wide-lane UPD value for GPS, between the 24th and 26th of July 2022. The main objective of this test was to analyze the results of the whole solution from a cold start. The vertical line in Figure 3 emphasizes the 24 hours mark. The estimated values of each satellite have a slow convergence, but it is safe to say that after one day of processing the UPDs reach full convergence. It is widely known that using a Melbourne-Wübbena combination, a very stable Wide-lane ambiguities can be estimated. Nonetheless, we experienced a slow convergence, which is expected due to the characteristics of the network algorithm. The convergence analysis was an important aspect of the development process, however it will not affect the end-user, as the solution is constantly running in near real-time and the cold start will only be present during the deployment phase or a restart.

The convergence of the UPDs can also be seen in Figure 4, which represents the standard deviation of the UPDs of each satellite. All the standard deviations stabilize under 0.01 WL cycles just before 24 hours of processing. Figure 5 shows the number of base stations used in the UPD estimation for each satellite. During the convergence phase, the network algorithm gradually

adds more bases until reaching a stable max number around the 24 hours timestamp. Finally, Figure 6 contains the probability density function (PDF) of the residual between the fix and float WL ambiguities. The two vertical lines represent the  $\pm 0.25$  cycles, so the residuals are below one quarter of a WL cycle.

As seen in Figures 3, 4, 5 and 6. The UPD values are very stable overtime, which indicates the quality of the estimation. The quality of this products will be validated using them in a user PPP-AR algorithm as shown in a later section of this paper.

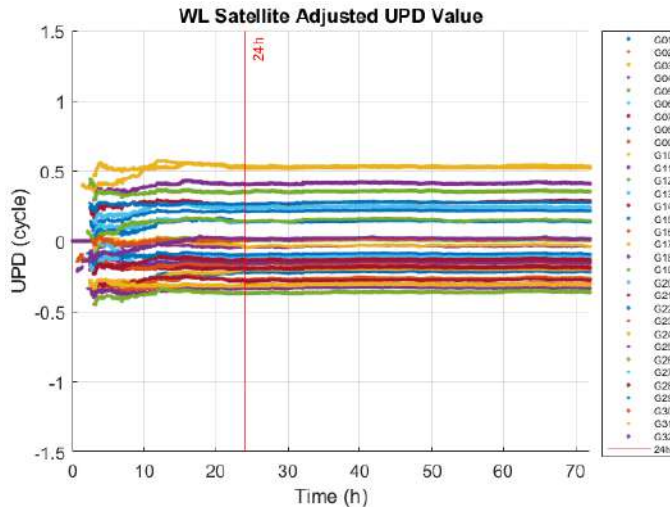


Figure 3: UPD WL GPS.

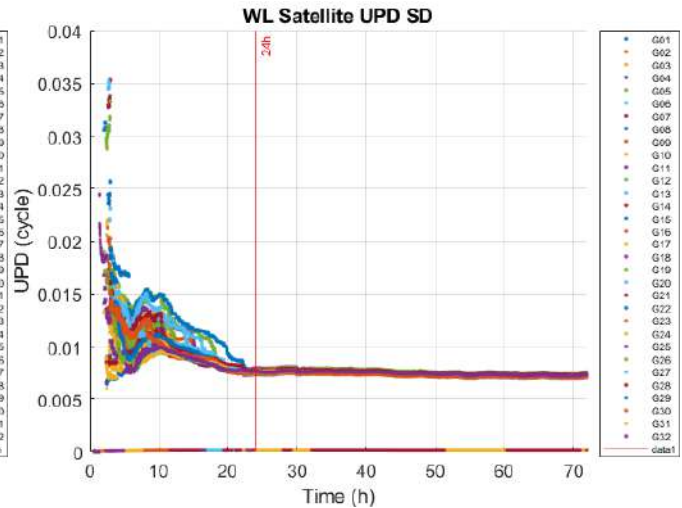


Figure 4: UPD WL GPS Standard Deviation.

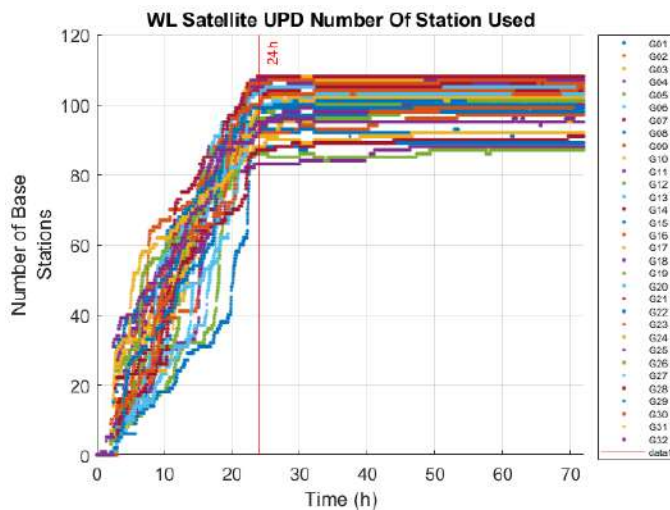


Figure 5: UPD WL GPS Number of Stations Used.

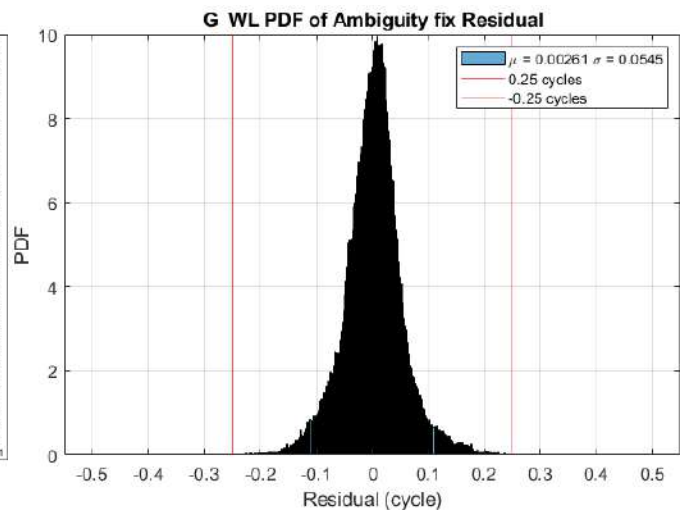


Figure 6: UPD WL GPS PDF.

## 2. UPD WL Galileo

Similarly to the previous section, the UPD values of Galileo were estimated between the 24th and 26th of July 2022. Figure 7 represents the UPD WL values of Galileo. These values are very stable, and the convergence seen at the very beginning of Figure 3 for the GPS is not present in this case.

Evidence of the full convergence around the 24 hours mark can be seen in Figure 8. After convergence, the standard deviations for all the Galileo satellites are 0.005 WL cycles, even lower than GPS. Interesting, the number of base stations used for each satellite UPD's estimation does not increase as fast as GPS. Even so, the quality of the values is still very high and can compare directly with GPS as it is clearly seen in Figure 10, were the PDF of the residual between the fix and float ambiguities is considerably smaller than one quarter of a cycle.

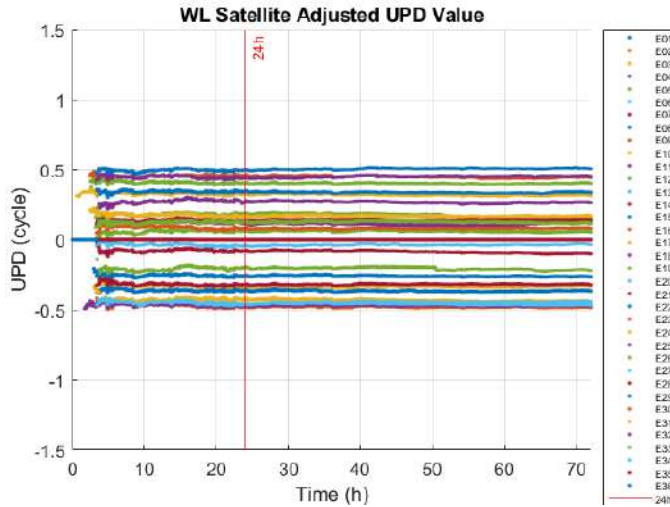


Figure 7: UPD WL Galileo.

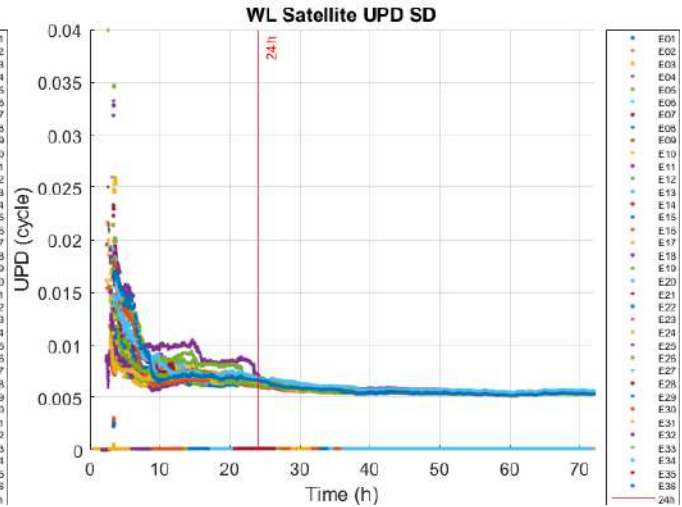


Figure 8: UPD WL Galileo Standard Deviation.

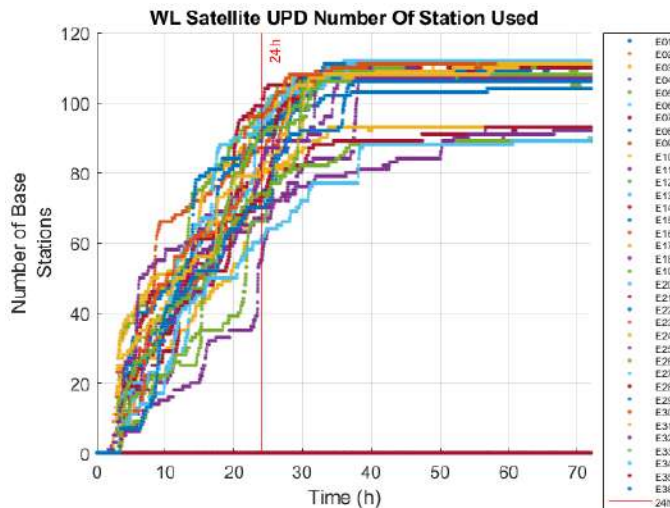


Figure 9: UPD WL Galileo Number of Stations Used.

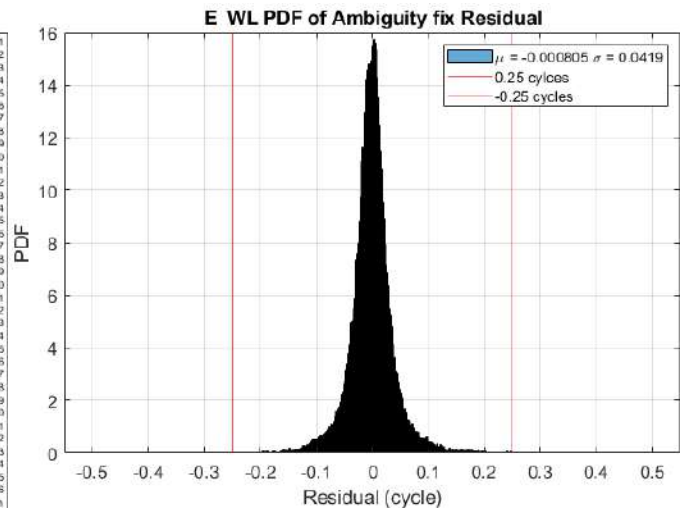


Figure 10: UPD WL Galileo PDF.

### 3. UPD NL GPS

Figure 11 shows the Narrow-lane UPD values of GPS. As before, the solution was tested between the 24th and 26th of July 2022. In this case, the results are considerably different from the ones seen for the WL (Figures 3 and 7). The convergence and stability of the UPD NL are not as good as previously seen, but this is expected given the different behaviors between the WL and NL ambiguities. For the UPD NL, not only the network estimator is responsible of the slow convergence, as the NL ambiguity takes additional time to convergence in the float ambiguity module of the solution.

Figure 12 represents the standard deviation of the products. Firstly, an initial gap between  $t = 0$  and  $t = 10$  hours can be seen. During this period, no UPD values are estimated as the Float ambiguities needed are not completely stable. This effect is part of the design and can be attributed to one of many parts of the integrity monitoring of the solution, as a non-stable float ambiguity used in the UPD estimation phase can introduce a bad initialization and very undesired results. This initial delay in the UPD estimation results in a convergence exceeding the 24 hours timestamp. Additionally, the standard deviation of all satellites increases between  $t = 55$ h and  $t = 70$ h. To understand this behavior, we can use Figure 13 to see the number of base stations used in the estimation of the UPDs of each satellite. A small decrease of base stations is experience during this same period, explaining the oscillation in their standard deviations. Finally, Figure 14 indicates the PDF of the residual float-fix for the NL ambiguity. Evidently, the residuals are not as sharp as in the case of the WL, but they are still of a very good quality as most of the residuals are less than one quarter of a cycle.

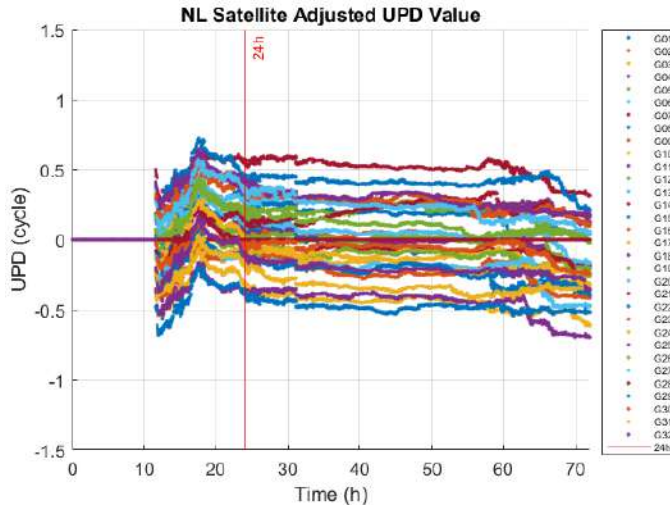


Figure 11: UPD NL GPS.

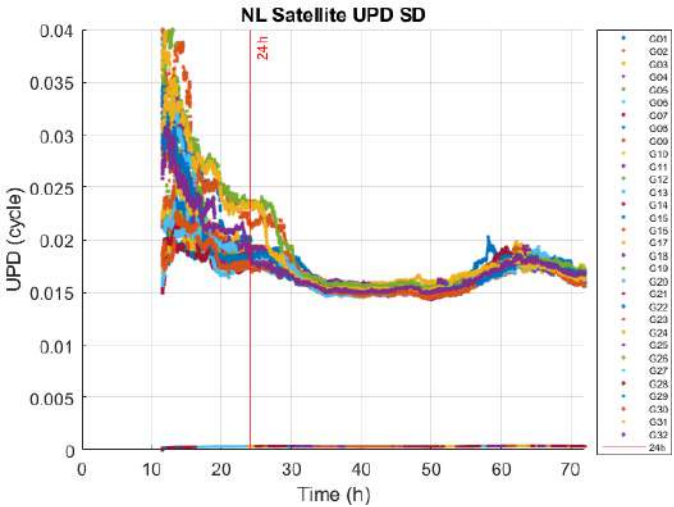


Figure 12: UPD NL GPS Standard Deviation.

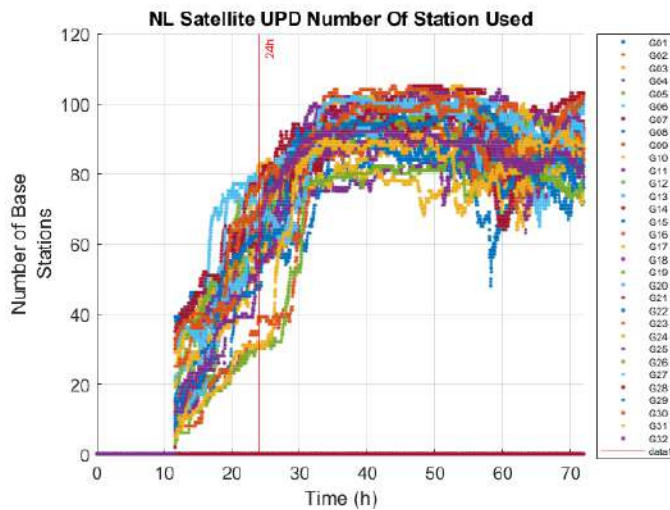


Figure 13: UPD NL GPS Number of Stations Used.

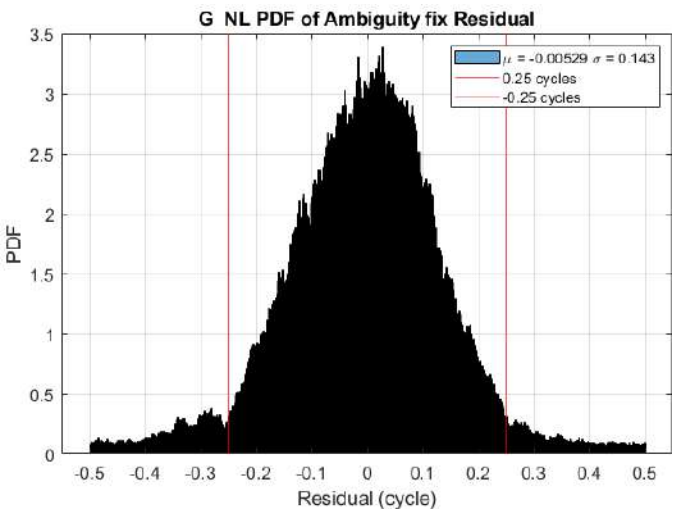


Figure 14: UPD NL GPS PDF.

**4. UPD NL Galileo**

Concerning the NL UPD for Galileo, the estimated values are displayed in Figure 15. The initial gap experienced in Figure 11 is larger in this case, which can be in part explained by the lower number of Galileo satellites. However, the UPD values converge around the same time as the initial convergence is smoother. Figure 16 shows the standard deviation of the UPD NL for Galileo, while Figures 17 and 18 expose the number of base stations used for each satellite’s estimation and the PDF of the residual fix-float ambiguity respectively. As before, the PDF of the residuals is smaller than one quarter of a cycle, which is a good indicator of the quality of the products.

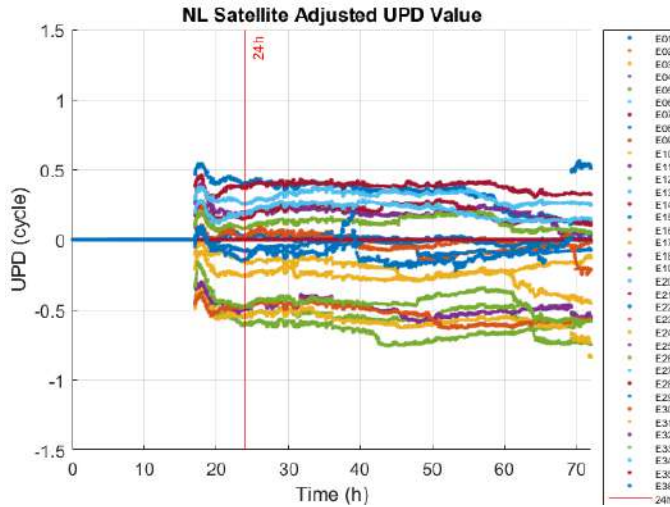


Figure 15: UPD NL Galileo.

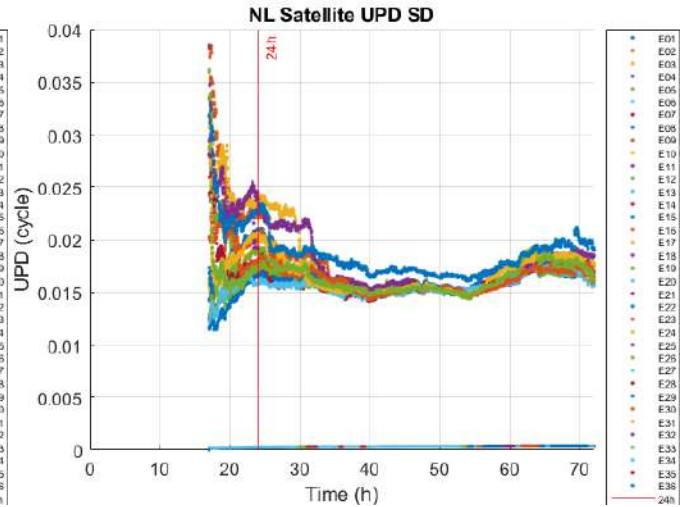


Figure 16: UPD NL Galileo Standard Deviation.

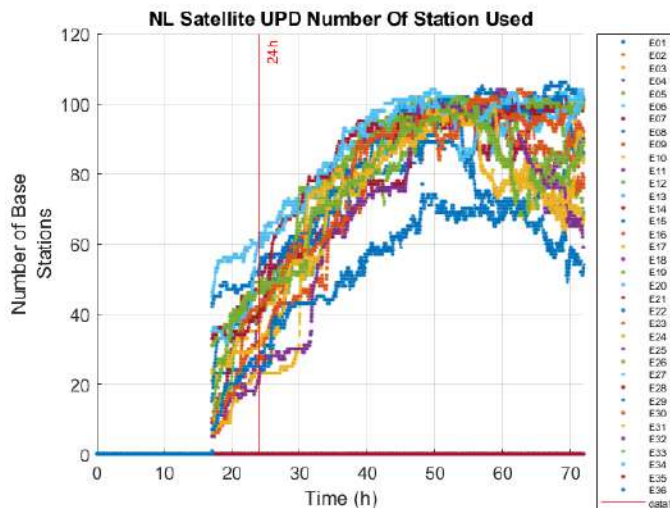


Figure 17: UPD NL Galileo Number of Stations Used.

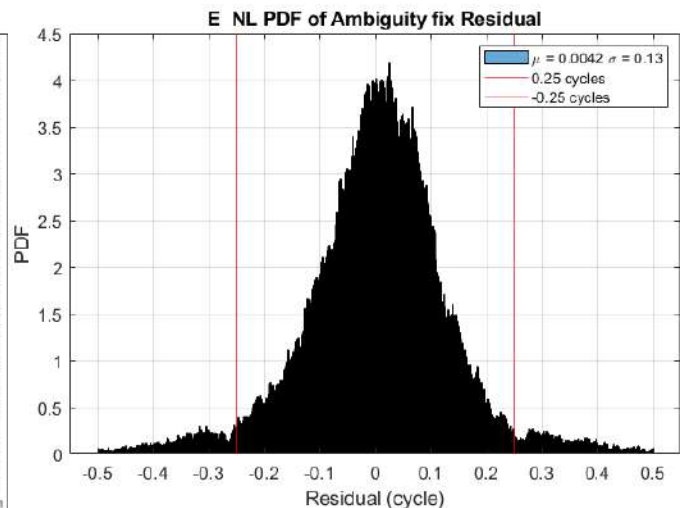


Figure 18: UPD NL Galileo PDF.

### 5. Integrity Monitoring and Quality Control with PPP-AR

To guarantee the quality and performance of the results presented in the previous section, a PPP with ambiguity resolution using the generated products is implemented. For the following test, a subset of base stations has been selected to constantly control the quality of the products. A high precision position for all the tested base stations in previously known, so the position error and the ambiguity status can be analyzed.

#### a) ABMF

The first base station tested was ABMF. Figure 19 represents the position error in the NED frame compared to a high precision reference. For the North and East components, the difference between the estimated position and the reference is always under 5cm after convergence.

Figure 20 shows the general satellite information. For the GPS constellation, the total number of satellites, as well as the number of fixed and rejected are shown with blue, green and red lines respectively.

Figure 21 presents the detailed information of each GPS satellite. The PRN of each satellite is presented in the y axis, and the same color code indicates the status of each satellite overtime. Green defines the fixed satellites, orange the float ones and red the rejected ones.



**Figure 19:** Base Station AMBF : Position Error



**Figure 20:** Base Station AMBF : General Satellite Information

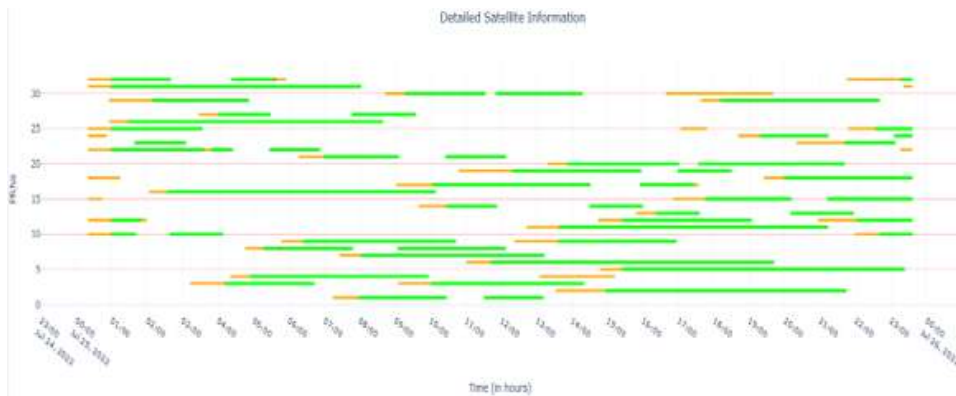


**Figure 21:** Base Station AMBF : Detailed Satellite Information

*b) ALIC*

The second base station used in the control group was ALIC. Figure 22 shows the position error for the North and East components. In this case, the difference between the estimated position and the reference is even smaller than in the first test, with an error always below 2cm after convergence.

Figure 23 indicates the total number of satellites used in the PPP, as well as the total number of fixed satellites at any given time. More details about the status of each satellite can be seen in Figure 24, where the precise status of each satellite is presented over time, the green, orange, and red lines represent the fixed, float and rejected satellites respectively.



**Figure 22:** Base Station ALIC : Position Error

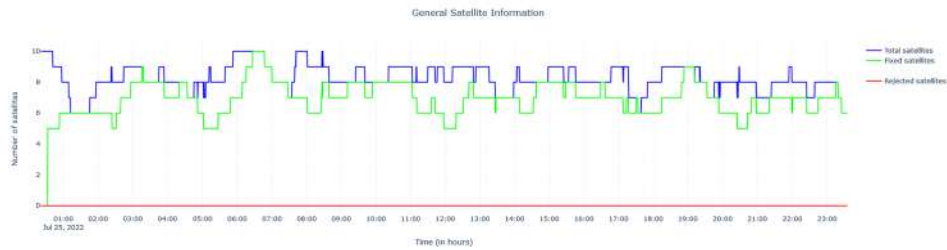


**Figure 23:** Base Station ALIC : General Satellite Information

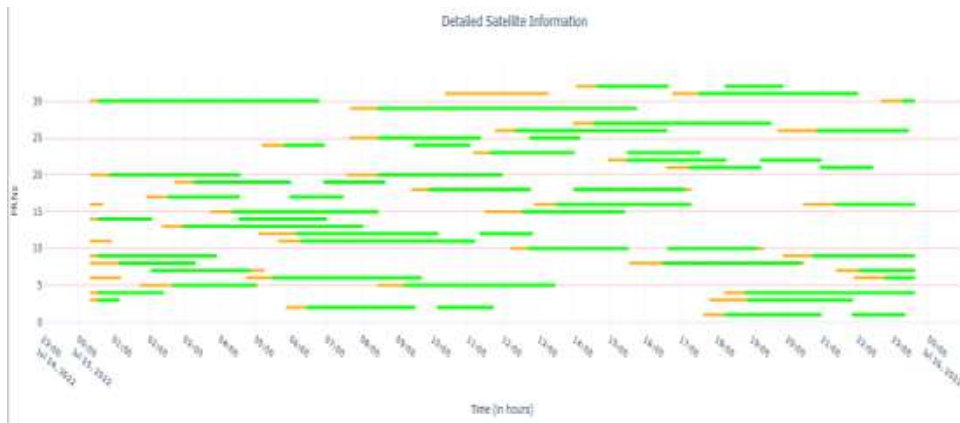


**Figure 24:** Base Station ALIC : Detailed Satellite Information

*c) CEDU*

The final base station used for the validation process was CEDU. Figure 25 introduces the position error in the NED frame. The results are very similar to the previous two cases, we have a centimeter-level error in both horizontal components. Figures 26 and 27 contain the general and detailed satellite information respectively. In both cases, the same color code is used, green indicates the fixed satellites, orange the float ones and red the rejected ones.

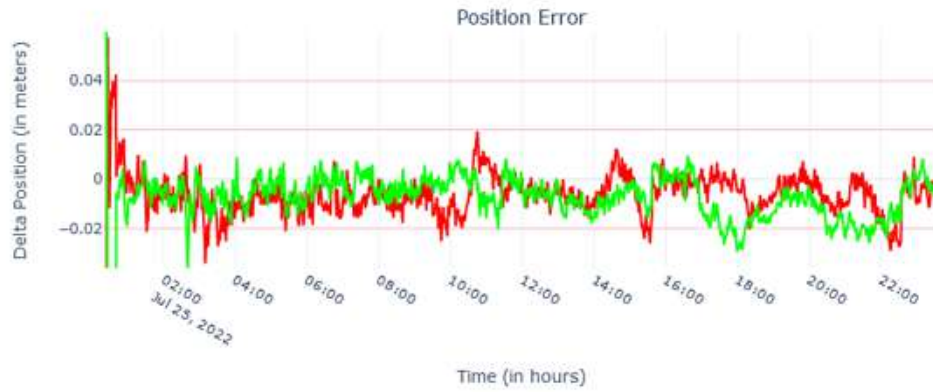


**Figure 25:** Base Station CEDU : Position Error



**Figure 26:** Base Station CEDU : General Satellite Information

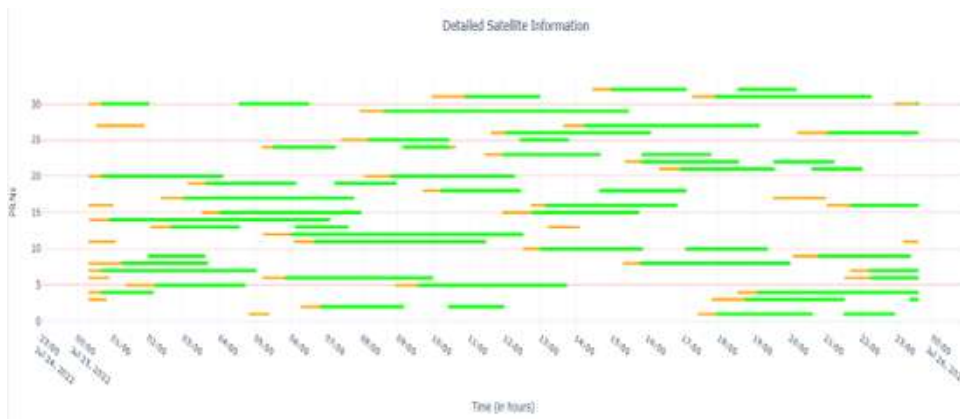


**Figure 27:** Base Station CEDU : Detailed Satellite Information

**6. Summary**

The performances obtained in the previous section are summarized in Table 1. The horizontal and vertical RMSs and 95th percentiles are at a centimeter level precision for all the three controlled base stations.

	Horizontal		Vertical	
	RMS [m]	95th percentile [m]	RMS [m]	95th percentile [m]
ABMF	0.0170	0.0328	0.0423	0.0677
ALIC	0.0106	0.0172	0.0345	0.0528
CEDU	0.0148	0.0254	0.0424	0.0844

**Table 1:** Results Summary

### 7. Near Real Time Visualizers

The main interest of the proposed solution is to provide the UPDs to the final user in near real time. This implies, that a quality control and monitoring of the solution must be performed at the same frequency. Several Graphical User Interfaces (GUI) were developed to visualize, debug, investigate and validate the estimated UPDs in real-time.

In Figure 28, the visualizer for the UPD WL products is presented. The UPD values are displayed intermediately after computation, allowing a visual scan and validation of the performance of the solution. Moreover, the historical date is also available, so the user can select any previous date to check the stability of the products before using them, or as an analysis tool after the mission. Additionally to the UPD values, their corresponding standard deviation and number of used base stations is showed. This information may be important to clarify the quality of the products and even detect potential problems by the data providers.

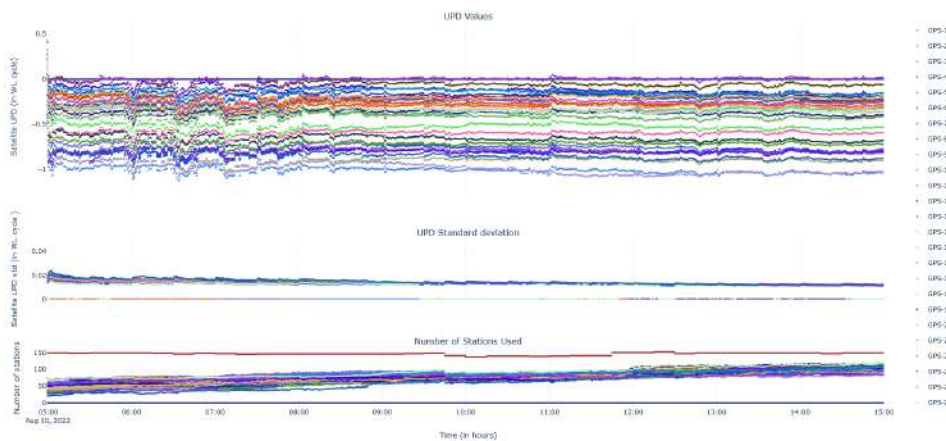


**Figure 28:** UPD WL Visualizer

Another important aspect of the solution is to provide a global coverage for the end-user. To guarantee this, the network of base stations used must be well scattered. The visualizer presented in Figure 29 was design to analyze and validate the network arrangement at any given time. Furthermore, this view indicates the reference base station that was used to separate the receiver and satellite biases.

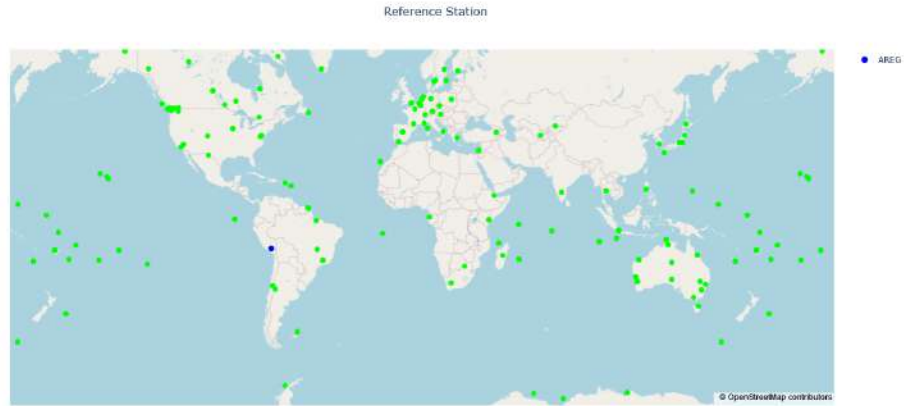


**Figure 29:** Network Visualizer

Finally, Figures 30 and 31 represent the network level satellite information for GPS and GALILEO respectively. These visualizers serve as a summary for the control stations per satellite and per epoch. Each satellite gives key information such as the number of stations observable from, the number of stations that either fixed, rejected or kept it as float (in green, orange, and red respectively).

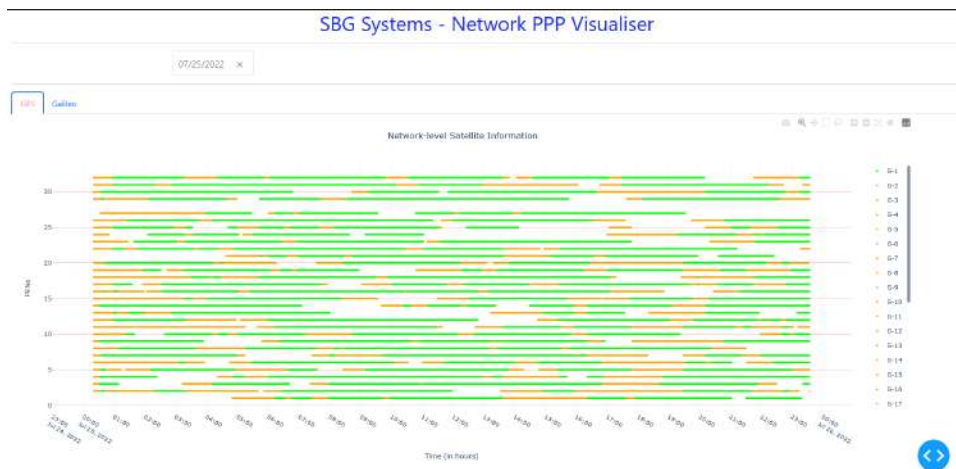


**Figure 30:** Visualizer: Network Level GPS Satellites Information

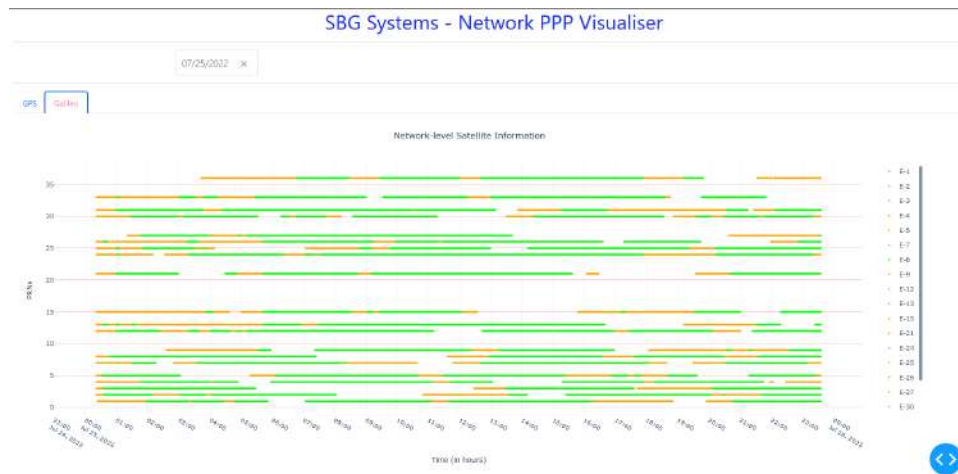


**Figure 31:** Visualizer: Network Level GALILEO Satellites Information

#### IV. CONCLUSIONS

We have developed an in-house solution that guarantees a centimeter-level position accuracy in near real-time mode. By having a complete hand from network to rover, we were able to prove the stability and consistency of the UPDs delivered. At each module, several integrity checks are performed to ensure that each data entry and exit is of good quality. The next objective will be to extend the solution to BeiDou and provide absolute UPDs for well-known frequencies which are needed for zero difference PPP.

**REFERENCES**

- [1] J. Zumberge, M. Heflin, D. Jefferson, M. Watkins, and F. Webb, "Precise point positioning for the efficient and robust analysis of gps data from large networks," *Journal of Geophysical Research*, vol. 102, 04 1997.
- [2] D. Laurichesse, F. Mercier, J.-P. Berthias, P. Broca, and L. Cerri, "Integer ambiguity resolution on undifferenced gps phase measurements and its application to ppp and satellite precise orbit determination," *Navigation*, vol. 56, pp. 135–149, 06 2009.
- [3] P. Li, X. Zhang, and F. Guo, "Ambiguity resolved precise point positioning with gps and beidou," *Journal of Geodesy*, vol. 91, 07 2016.
- [4] D. Laurichesse and S. Banville, "Instantaneous centimeter-level multi-frequency precise point positioning," *GPS World*, 07 2018.
- [5] X. Li and X. Zhang, "Improving the estimation of uncalibrated fractional phase offsets for ppp ambiguity resolution," *Journal of Navigation*, vol. 65, 07 2012.
- [6] J. Hu, X. Zhang, P. Li, F. Ma, and L. Pan, "Multi-gnss fractional cycle bias products generation for gnss ambiguity-fixed ppp at wuhan university," *GPS Solutions*, vol. 24, 11 2019.
- [7] X. Li, X. Han, X. Li, G. Liu, G. Feng, B. Wang, and H. Zheng, "Great-upd: An open-source software for uncalibrated phase delay estimation based on multi-gnss and multi-frequency observations," *GPS Solutions*, vol. 25, 04 2021.
- [8] D. Gallego Maya, R. Zaid, K. Y. Kouedjin, P. Sarri, and A. Guinamard, "Tightly coupled integration of inertial data with multi-constellation ppp-if with integer ambiguity resolution," *Proceedings of the 34th International Technical Meeting of the Satellite Division of The Institute of Navigation (ION GNSS+ 2021)*, vol. 56, pp. 2879 – 2894, 09 2021.
- [9] X. Li, X. Li, G. Liu, X. Weiliang, F. Guo, Y. Yuan, K. Zhang, and G. Feng, "The phase and code biases of galileo and bds-3 boc signals: effect on ambiguity resolution and precise positioning," *Journal of Geodesy*, vol. 94, 01 2020.
- [10] J. Wang, Q. Zhang, and G. Huang, "Estimation of fractional cycle bias for gps/bds-2/galileo based on international gnss monitoring and assessment system observations using the uncombined ppp model," *Satellite Navigation*, vol. 2, 12 2021.
- [11] G. Xiao, L. Sui, B. Heck, T. Zeng, and Y. Tian, "Estimating satellite phase fractional cycle biases based on kalman filter," *GPS Solutions*, vol. 22, 06 2018.